REPRODUCTIVE CHARACTER DISPLACEMENT AND SIGNAL ONTOGENY IN A SYMPATRIC ASSEMBLAGE OF ELECTRIC FISH

William G. R. Crampton,[1,2] Nathan R. Lovejoy,[3] and Joseph C. Waddell[1]

[1]Department of Biology, University of Central Florida, 4000 Central Florida Boulevard, Orlando, 32816-2368, Florida, USA

   [2]E-mail: crampton@mail.ucf.edu

[3]Department of Biological Sciences, University of Toronto Scarborough, 1265 Military Trail, Toronto, ON M1C 1A4, Canada

The reproductive signals of two or more taxa may diverge in areas of sympatry, due to selection against costly reproductive interference. This divergence, termed reproductive character displacement (RCD), is expected in species-rich assemblages, where interspecific signal partitioning among closely related species is common. However, RCD is usually documented from simple two-taxon cases, via geographical tests for greater divergence of reproductive traits in sympatry than in allopatry. We propose a novel approach to recognizing and understanding RCD in multi-species communities—one that traces the displacement of signals within multivariate signal space during the ontogeny of individual animals. We argue that a case for RCD can be made if the amount of signal displacement between a pair of species after maturation is negatively correlated to distance in signal space before maturation. Our application of this approach, using a dataset of communication signals from a sympatric Amazonian assemblage of the electric fish genus *Gymnotus*, provides strong evidence for RCD among multiple species. We argue that RCD arose from the costs of heterospecific mismating, but interacted with sexual selection—favoring the evolution of conspicuous male signals that not only serve for mate-choice, but which simultaneously facilitate species recognition.

KEY WORDS: Electrocommunication, *Gymnotus*, masking interference, reinforcement, sexual selection, signal partitioning.

Where closely related species occur in sympatry, selection may result in the divergence of signals related to reproduction (Howard 1993; Butlin 1995; Servedio and Noor 2003; Pfennig and Pfennig 2009). This phenomenon, often referred to as reproductive character displacement (RCD) (Howard 1993), is thought to result from selection against costly reproductive interactions among heterospecifics (reproductive interference, sensu Gröning and Hochkirch 2008). One type of reproductive interference involves heterospecific "mismating" events, arising from errors in recognition between species (or divergent populations) that possess similar mate attraction signals. Reinforcement is a predicted consequence of mismating between populations with incomplete postzygotic isolating mechanisms, where character displacement is driven by the costs of hybridization, for example, reduced hybrid fertility (Noor 1999; Servedio and Noor 2003). A related phenomenon, facilitated RCD (sensu Howard 1993), arises from mismating between fully fledged species that do not hybridize. In this case, character displacement is a postspeciation phenomenon driven by the costs of wasted time, energy, or gametes during attempts to attract, approach, or mate with heterospecific sexual partners (Endler 1989).

Another recognized type of reproductive interference is the phenomenon of masking interference, where spectral overlap between the signals of two species impairs the ability of either or both species to locate or communicate efficiently with conspecifics (Amezquita et al. 2006; Gröning and Hochkirch 2008). Unlike with selection against errors in mate recognition, for signals to diverge in response to masking interference, direct reproductive contact with consequent mismating is not necessary—accounting for why masking interference is often found among distantly related taxa that are unlikely to attempt to breed (e.g., Amezquita et al. 2006).

Although RCD has largely come to be defined as the geographical pattern of greater reproductive trait difference between taxa in sympatry compared to trait differences between the same taxa in allopatry (Howard 1993), we join others (Butlin and Ritchie 1994; Pfennig and Pfennig 2009) in considering RCD to be the process of divergence among sympatric taxa that can lead to this geographical pattern. In this article, we specifically define RCD as the process of signal divergence driven by the avoidance of reproductive interference (i.e., mismating and masking interference) between taxa in sympatry. As such we emphasize the distinction of RCD from alternative mechanisms of signal divergence that can lead to patterns of signal partitioning (i.e., nonoverlapping signal properties) among sympatric taxa. These include divergent sexual selection (e.g., Boul et al. 2007), sensory drive (e.g., Boughman 2002), selective pressures from predators (e.g., Ryan 1985), incidental correlation of signals with morphological traits exposed to ecological character displacement (e.g., Podos 2001), and nonadaptive drift (e.g., Gerhardt 1999). In these cases, signal divergence is not a result of selection to minimize costly reproductive interactions, and a pattern of enhanced trait divergence in sympatry versus allopatry is not expected.

Based on the geographical test of differences in reproductive traits in sympatry compared to allopatry (see Fig. 1), RCD of mate attraction signals has been proposed for pheromonal, acoustic, and visual communication systems in insects, anurans,

reptiles, and birds (reviews in Howard 1993; Butlin 1995; Noor 1999; Cooley 2007; Gröning and Hochkirch 2008; Pfennig and Pfennig 2009). These studies are nearly always based on two-taxon systems where the investigations are minimally impacted by interactions with additional closely related sympatric species (an exception is Lemmon 2009, which considered a zone of tri-sympatry). These simple systems serve as natural laboratories—permitting a controlled test of the theoretical expectations of RCD. However, there is no reason why reproductive interference should not induce RCD among the signals of multiple species in a diverse sympatric community—where it is common to observe species-specific partitioning of mating signals.

SIGNAL PARTITIONING AND RCD IN MULTISPECIES COMMUNITIES

Many studies of diverse tropical communities have documented patterns of signal partitioning, where taxa exhibit distinct, species-specific signals with nonoverlapping spectral and/or temporal properties. Most cases have been documented from the acoustic signals of anurans and birds in polyphyletic continental assemblages (e.g., Nelson 1989; Wollerman 1999; Luddecke et al. 2000; Chek et al. 2003; Amezquita et al. 2006; Luther and Wiley 2009). Some of these studies interpreted signal partitioning as a response to mismating between heterospecifics with confusingly similar calls, that is, facilitated RCD (e.g., Nelson 1989; Wollerman 1999; Luther and Wiley 2009). Others noted nonoverlapping ranges of the dominant signal frequencies among species, and interpreted these as a response to masking interference. Signal partitioning has also been documented in monophyletic species flocks that diverged rapidly in insular circumstances, for example, acoustic calls in crickets (Otte 1994; Mendelson and Shaw 2005), color in cichlid fish (e.g., Allender et al. 2003; Seehausen et al. 2008), and electric signals in mormyrid fish (e.g., Hopkins 1999; Arnegard and Hopkins 2003; Arnegard et al. 2005, 2010a; Feulner et al. 2006). Some of these studies speculated that signals diverged concomitant with speciation in response to sexual selection (but with a possible role for reinforcement) (e.g., Mendelson and Shaw 2005; Feulner et al. 2006; Arnegard et al. 2010a).

In the absence of geographical (or other) tests, we contend that most studies of community-wide signal partitioning can only speculate a role for RCD in explaining why signals are divergent. Geographical tests for RCD involving multiple species from local or regional assemblages are, nonetheless, seldom attempted. An exception is Otte's (1994) monographic study of a Hawaiian cricket species flock, which documented RCD from a small subset of species pairs with identified zones of allopatry. However, simultaneous documentation of the strength and magnitude of RCD among all, or even most, pairs of species in a diverse local community has not been attempted using geographical trait comparisons. We argue that the geographical approach to testing for RCD
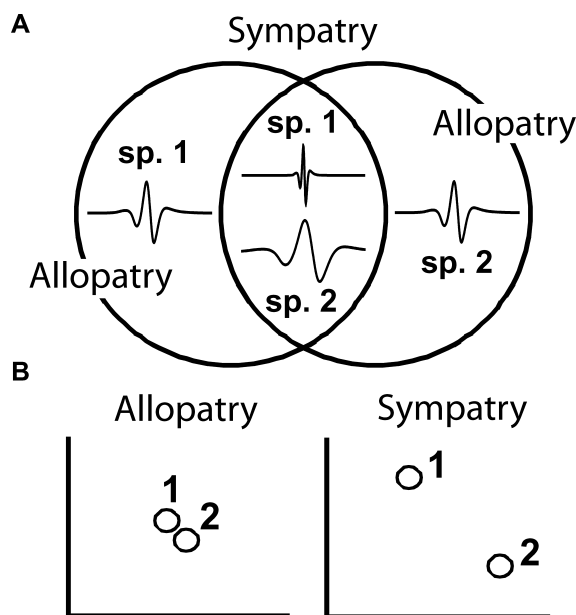

Figure 1. The geographical test for reproductive character displacement. (A) Mate attraction signals (illustrated here by electric fish time-voltage waveforms) exhibit displacement in sympatry relative to allopatry. (B) Displacement is quantified by distance between species-centroids in a multivariate signal space (represented here as a two-dimensional ordination; circles are species-centroids).

among multiple (3+) species in a community may be intractable because it requires characterizing disparities in signal traits among populations in zones of both sympatry and allopatry—not only for a potentially large number of pairwise combinations of species (e.g., for seven species there are 21), but also over a geographical area that may extend far outside the community under study. In continental systems of the humid tropics, species ranges are often large (Crampton 2011), and distributions rarely known well enough to identify zones of allopatry with certainty.

Unique among studies of community-wide signal partitioning in employing an alternative (nongeographic) test for RCD, is Chek et al's (2003) survey of acoustic communication in anurans. Using a null model-based procedure, the authors reported patterns of over-dispersal and regularity of spacing in signal parameters, for some communities, and interpreted these patterns as evidence for a history of selection against reproductive interference (i.e., RCD). They contrasted these observations with cases in which signals exhibited partitioning but not structured spacing—a pattern that could readily arise from divergence in allopatry preceding contact in sympatry (see Mayr 1988), or drift following contact. Chek et al. (2003) noted that community-wide signal partitioning is uncommon in anuran assemblages, occurring only where signal space is crowded, and typically involving both overdispersion of dominant frequency (consistent with a hypothesis of divergence driven by selection against masking interference), and also pulse rate (consistent with selection against mismating).

AN ONTOGENETIC TEST FOR RCD IN MULTISPECIES COMMUNITIES

Here we propose an alternative procedure for recognizing RCD in multispecies communities—one based on expected patterns of ontogenetic changes in signal structure. Just as a geographical pattern of trait divergence can be indicative of RCD (Fig. 1), we suggest that an ontogenetic pattern of trait change can also provide evidence for RCD. Our procedure is based on a mathematically expressible set of expectations in which we argue that a strong case for RCD can be made if the amount of signal displacement between a given pair of species after maturation is negatively correlated to how different the signals were before maturation. In other words, we posit that the more similar two species' signals are at the immature stage, the further they should be pushed apart by RCD. We then apply this test to an ontogenetic series of electric signals from a species-rich sympatric assemblage of the weakly electric Neotropical freshwater knife fish genus, *Gymnotus* (Gymnotiformes). These nocturnally active fish generate stereotyped, pulsed, weak (<2 V) electric organ discharges (EODs), which in combination with cutaneous electroreceptors, serve two functions: the detection of nearby objects (electrolocation), and communication, including mate-attraction (Albert and Crampton 2005; Bullock et al. 2005). These EODs are first generated a few days after hatching, and thereafter undergo distinct ontogenetic changes throughout growth and maturation (Crampton and Hopkins 2005; Pereira et al. 2007).

Methods

A TEST FOR RCD BASED ON SIGNAL ONTOGENY

Our test requires that the subjects' signals can be captured digitally and mapped into a continuous multivariate signal space representing signal structure (sensu Nelson and Marler 1990), within which distances between species can be measured quantitatively. The concepts of our test are outlined in Figure 2. Here, signal variation is illustrated by the shape of time-voltage waveforms resembling EODs. We employ the squared Mahalanobis distance (D^2) as a metric of distance between the centroids of groups of individuals in multivariate signal space. First, the signals of each species must be divided into at least three ontogenetic stages, with only the last representing mature individuals. For instance, for stages A, B, and C (Fig. 2A), the transition from A to B represents growth, whereas the transition from B to C represents maturation. Next, for N sympatric species we consider the distances in signal space between all $((N^2 - N)/2)$ combinations of species pairs. For each species pair, we then define i as the distance between the centroids of the pair before an ontogenetic transition and j as the distance after the transition. Finally, we plot i as the predictor variable and j/i (the proportional change in distance attending a transition) as the response variable (Fig. 2C.ii). We will henceforth use the term "ontogenetic signal displacement" to refer to j/i. Because our test is based on determining a statistically significant regression from multiple values of i and j/i (i.e., multiple species pairs), it is constrained to multispecies assemblages. To clarify how the test works, below we consider a case in which the signals of sympatric species do not change during an ontogenetic transition, followed by a case of RCD.

Stasis in signal space

Under conditions of stabilizing selection, random drift in signal space, or due to developmental constraints on signal design (as might be expected during some parts of growth), D^2 between a pair of species should, on average, neither increase nor decrease during an ontogenetic transition. Thus, we expect a regression of i versus j to exhibit a linear function of the form $j = i$ over the full range of i (Fig. 2C.i). This can otherwise be represented as a nonsloped "linear" function (significant intercept but not slope) of the form $j/i = 1$ in a plot of i versus j/i (Fig. 2C.ii).

RCD

For explanatory purposes, we consider here only the transition from immature adults to mature males, and we assume that RCD involves selection against mismating. If the signals of two species
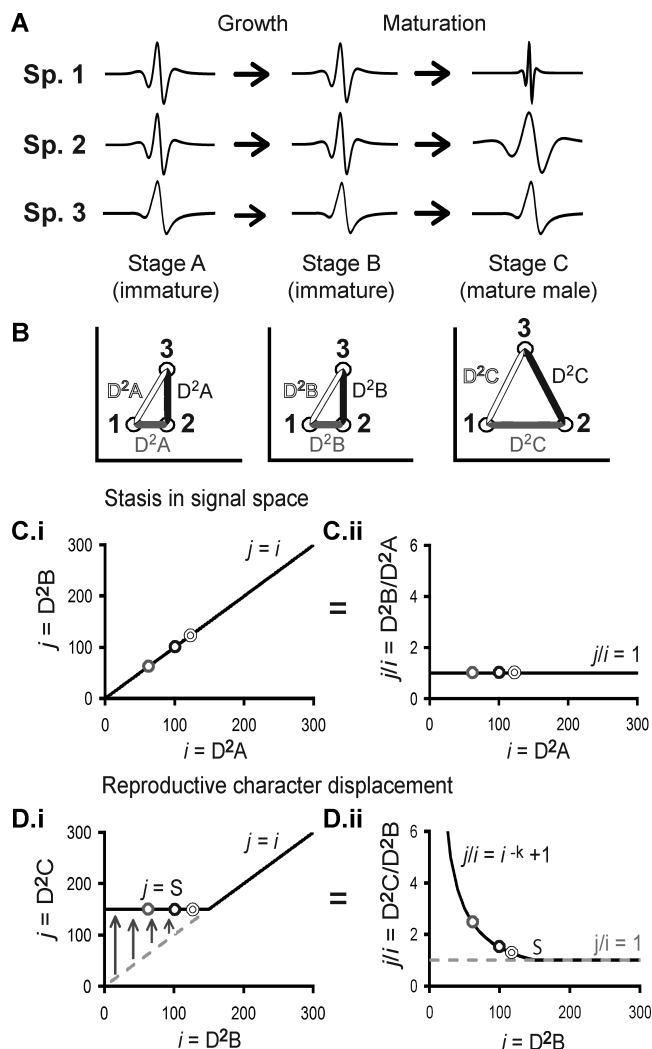
Figure 2. An ontogeny-based test for reproductive character displacement (RCD) of mating signals in a multi-species assemblage. (A) Ontogeny of signals of three species (represented by electric fish signals). (B) Two-dimensional ordination of signal space for the signals in (A), with circles as species-centroids, and the squared Mahalanobis distances (D^2) between species pairs identified by black, gray, and white lines. (C and D) Expected regression of D^2 between species pairs before an ontogenetic transition (*i*) versus after the transition (*j*) (expressed alternatively, to right, as *i* vs. *j/i*) under conditions of stasis in signal space (C) and RCD (D). The black, gray, and white circles correspond to the three D^2 distances in B. The vertical arrows in D.i represent the strength of selection for signal divergence.

are nearby in signal space before maturation (D^2 is small), then unless the signals of males diverge during maturation, the risk of mismating is high—predicting strong selection for signal divergence. Therefore, in this example, a large displacement of signals during maturation is consistent with a history of RCD. Conversely, if two species are already well-spaced prior to maturation (D^2 is large), there is a lower risk of mismating—predicting a smaller displacement of signals during maturation. Accordingly, under

conditions of RCD we predict a negative correlation between *i* and *j/i*.

We refine this test by also assuming that the risk of mismating will decline with increasing D^2 between male signals until a "safe distance" (S) is reached, beyond which additional increases in D^2 will not yield additional reductions in the probability of mismating. Therefore, we expect a piece-wise function (Fig. 2D.i) where: if *i* < S we expect *j* to be pushed toward S, but if *i* > S, we expect *j* = *i*. In Figure 2D.i we illustrate selection for signal divergence in response to mismating (i.e., RCD) as vertical gray arrows; longer arrows indicate stronger selection. Here, selection strength, and thus the predicted response, ontogenetic signal displacement (*j/i*, as depicted in Fig. 2D.ii), declines in the form of a negative asymptotic power function from a maximum where *i* is very small, to negligible levels where *i* = S. In sum, under conditions of RCD we predict an asymptotic negative power function of the form $j/i = i^{-k} + 1$, where the asymptote (*j/i* = 1) is approached at *i* = S (Fig. 2D.ii).

THE MODEL SYSTEM—*GYMNOTUS* OF THE CENTRAL AMAZON

Our study is based on an assemblage of *Gymnotus* documented within 50 km of the town of Tefé, Brazil (3°20′45″S, 64°42′36″W), in the lowland Central Amazon (Fig. S1). During a seven-year period of multiseason and multihabitat fieldwork, 12 sympatric species of *Gymnotus* were documented from this area (Crampton 2011). Four of these, *G. carapo*, *G. melanopleura*, *G. onca*, and *G. tigre*, are excluded from this study because they were documented from single or small numbers of immature specimens, and may be vagrants. The remaining eight species form breeding populations (*G. arapaima*, *G. coatesi*, *G. coropinae*, *G. curupira*, *G. jonasi*, *G. mamiraua*, *G. obscurus*, *G. varzea*). All eight are genetically distinct species whose phylogenetic positions are known (Lovejoy et al. 2010). *Gymnotus obscurus* was included in descriptive analyses, but excluded from our ontogenetic test for RCD because it retains the biphasic EOD typical of larval *Gymnotus* (Crampton and Hopkins 2005; Pereira et al. 2007) throughout ontogeny—placing adults in a far-outlying position in signal space relative to congeners (see Results). Therefore, although we describe signal ontogeny for eight species, only seven of these are included in our test for RCD.

In the Tefé region, *Gymnotus* occur in three ecosystems (Crampton and Albert 2006; Fig. S1): (1) the floodplains of nutrient-rich (conductivity ca. 80–150 µScm⁻¹) whitewater rivers; (2) the floodplains of nutrient-poor (ca. 5–30 µScm⁻¹) blackwater rivers, and; (3) nutrient-poor (ca. 5–30 µScm⁻¹) forest streams and adjacent ephemeral swamps draining terra firme lowland formations lying above river-floodplain systems. Three of the resident species are restricted to terra firme systems (*G. coatesi*, *G. coropinae*, *G. curupira*), four are restricted to

whitewater floodplains (*G. jonasi*, *G. mamiraua*, *G. obscurus*, and *G. varzea*), and one, *G. arapaima*, is eurytopic—occurring in all three habitats (Crampton and Albert 2006). Nests containing postlarval and small juvenile individuals guarded by a single male (see Crampton and Hopkins 2005 for *G. mamiraua*), were found for four species, permitting species identification and EOD recordings of the postlarval ontogenetic stage.

SEX AND ONTOGENETIC STAGES

Sex was assessed by dissection under a stereomicroscope. Reproductively mature specimens (gonads at Nikolsky stages 2–4, Appendix S1) were divided into males (M) and females (F). Immature specimens (Nikolsky stages 0–1) were divided into four stages: J0 = postlarval; J1 = small juvenile; J2 = large juvenile; IA = immature adult. We defined immature adults as immature specimens exceeding the minimum total length for reproductively mature specimens of the same species. The length cut-offs between stages J0 and J1, and between J1 and J2, were defined by putatively homologous morphological landmarks (Appendix S2, Fig. S2). We recorded EODs from 42 of the 48 combinations of eight species and six ontogenetic categories.

ELECTRIC SIGNAL RECORDINGS

Fish were recorded within 48 h of capture in a nylon mesh envelope suspended in the center of an 88×37 cm insulated tank filled to a depth of 34 cm (114-L cooler). Water temperature was standardized to $27.0 \pm 0.1°$C, and conductivity to $55 \pm 1\ \mu\mathrm{Scm}^{-1}$. Recordings were made from at least 1 h after sunset to 0300 h, in near-darkness, following acclimation in the tank for 5–15 min. Single head-to-tail EOD recordings were taken from tank-end Ag/Ag-Cl or NiCr electrodes, using an AC-coupled amplifier (DC – 30 kHz or 0.01 Hz–30 kHz), and digitized at 48–250 kHz (details in Appendix S3). Fish with damaged or regenerated tails were excluded. Following recordings, specimens were euthanized, fixed with 10% formalin, and measured for total length and weight before preservation in 70% ethanol.

DISCRETE WAVELET TRANSFORM (DWT)

We used the DWT to convert raw digitized EODs into a reduced number of signal features for multivariate analysis. DWT coefficients can represent efficiently both frequency and location (temporal) information in a digital signal; see Crampton et al. (2008) for a discussion of our choice of DWT over rival procedures. We used custom scripts in MATLAB version 7.1 (The Mathworks, Natick, MA), with commands from WaveLab 850 (http://www.stat.stanford.edu/~wavelab/) to generate a dimension-reduced matrix of 85 columns of DWT coefficients and 677 rows, each row representing an individual fish's EOD (details in Crampton et al. 2008; Appendix S4).

GRAPHICAL ORDINATION IN SIGNAL SPACE

To visualize the occupation of signal space by groups of *Gymnotus*, we subjected the 85×677 matrix of DWT coefficients characterizing EOD structure to linear discriminant analysis (LDA), assuming equal a priori probabilities of group membership for all groups. LDA scores were then subjected to principal component analysis to yield a two-dimensional plot of canonical scores for each individual EOD. These analyses were performed using a custom-written MATLAB program.

QUANTIFYING MULTIVARIATE DISTANCES IN SIGNAL SPACE

Our metric of distance in multivariate signal space, D^2, is a scale-invariant measure that takes into account the correlations of the covariance–variance matrix such that the distance between group centroids is weighted by the variance within and between groups (Mahalanobis 1936). Because of these properties, D^2 (or D) has been used in other evolutionary studies of trait distances (e.g., Cherry et al. 1982), including for electric fish signals (Arnegard et al. 2010a). We calculated D^2 between all 42 ontogenetic-species groups from the 85×677 matrix of DWT coefficients using a custom script in R version 2.9 (R Foundation). We used two procedures for representing changes in distances between pairs of species in signal space, during an ontogenetic transition.

Mode A (Fig. 3A) is the most direct means of testing for RCD, and is the basis for the schematic in Figure 2. In a transition from stage A to stage B (e.g., immature to mature), for *N* species, we pair $(N^2 - N)/2$ measurements of *i* (where *i* represents D^2 between the centroids of stage A individuals of a given species pair), with $(N^2 - N)/2$ calculations of *j/i* (where *j* represents D^2 between the centroids of stage B individuals of the same species pair). Mode A measurements in signal space are used for all the analyses presented in this paper, except for the analyses described in "Ranking species by averaged ontogenetic signal displacement from heterospecifics," where instead we employed Mode B.

Mode B (Fig. 3B): Although Mode A gives a single measure for the displacement of a pair of species in signal space, it does not provide information about the relative contribution of each species to the displacement (i.e., asymmetries in trait displacement). We designed Mode B to independently quantify the displacement of each member of a species pair during an ontogenetic transition. In a transition from stage A to stage B, for *N* species, we pair $(N^2 - N)/2$ separate measurements of *i* (where $i = D^2$ between the centroids of stage A individuals of a given species pair) with $(N^2 - N)$ separate calculations of *j/i*. Unlike in Mode A, a single value of *i* (e.g., solid gray line labeled *i* for species 1 and 2 in Fig. 3B) is represented by two independent measurements of *j*. In this case, first, the distance from stage B of species 2 (sp. 2B) to stage A of species 1 (sp. 1A) (dashed gray line "*j1*" in Fig. 3B, corresponding to gray circle 1 in lower plot), and; second, the
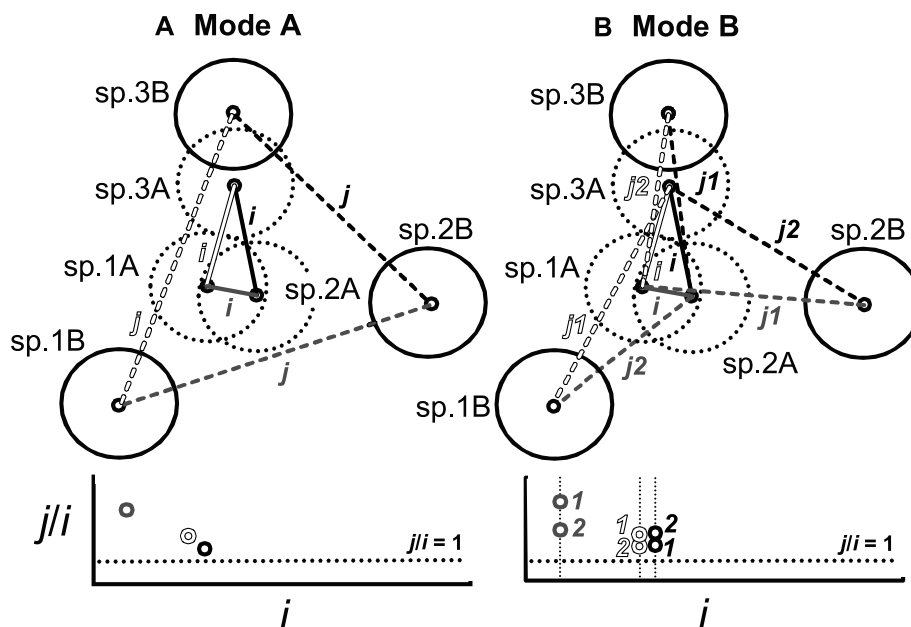
Figure 3. Procedures for representing character displacement in a signal space. In the upper plots, three species are represented by successive ontogenetic stages A (dashed circles) and B (solid circles). Inner circles are centroids. Measurements of *i* and *j* are represented by solid and dashed lines, respectively, with each species pair identified by shading (black, gray, or white, corresponding to the black, gray, and white circles in the lower plots). Dotted vertical lines in lower plot, for Mode B, recall that one value of *i* is associated with two values of *j/i* for each species pair.

distance from stage B of species 1 (sp. 1B) to stage A of species 2 (sp. 2A) (dashed gray line "*j2*," corresponding to gray circle 2 in lower plot).

BOOTSTRAPPING MEASUREMENTS OF D^2

To limit the possibility that the distances between group centroids (D^2) were biased by outlying individuals within any given group, we used a custom R script to perform a bootstrap procedure, in which we randomly resampled (with replacement) individual EODs within each of the 42 groups. For the final matrix of 85 DWT coefficients × 677 EODs, we conducted 1000 rounds of resampling, generating 1000 matrices across which we calculated the mean D^2 (with ±1 standard deviation) between all 42 groups. All D^2 values reported in this article refer to these bootstrapped means.

STATISTICAL TESTS FOR RCD

We adopted three complementary approaches to describe the relationship between the predictor variable (*i*) and response variable (*j/i*) during an ontogenetic transition, and disparities among these relationships. All analyses were performed using custom scripts in R. (1) For each plot of *i* versus *j/i* we fitted the following biologically plausible regressions using nonlinear or linear modeling: power + 1 (power function with asymptote at 1), power, linear, exponential, logarithmic, and logistic. Next, we used Akaike's information criterion (AIC) with a second-order correction (AICc)

to select the regression that best described the data. Where the AIC Evidence Ratio of no single function exceeded that of any other by more than twice, we inferred that there was no "best" model. In these cases, we assumed a linear model, and if the intercept (but not slope) was significant, we described the relationship as a "nonsloped linear" function. (2) We calculated the *P*-values for the slope and intercept of the regression derived from (1) (above). Here data were ln–ln transformed if the regression was nonlinear. (3) We used analysis of covariance (ANCOVA) to examine disparities in the strength of ontogenetic character displacement (relationship between *i* and *j/i*), with the covariate representing alternative ontogenetic transitions (e.g., immature adult to mature male vs. immature adult to mature female).

RANKING SPECIES BY AVERAGE ONTOGENETIC SIGNAL DISPLACEMENT FROM HETEROSPECIFICS

To measure the average amount of ontogenetic signal displacement (i.e., *j/i* in Fig. 2Dii) of a given species from all other heterospecifics (during maturation), we used Mode B measurements pertaining to the transition from immature adults to mature males (or females). For instance, to measure the proportional character displacement of male *G. arapaima* from *G. coatesi*, we defined *i* as D^2 from the centroid for immature adult *G. arapaima* to the centroid for immature adult *G. coatesi*. We then defined *j* as D^2 from the centroid for mature male *G. arapaima* to the centroid for immature adult *G. coatesi*. For each species, we repeated this
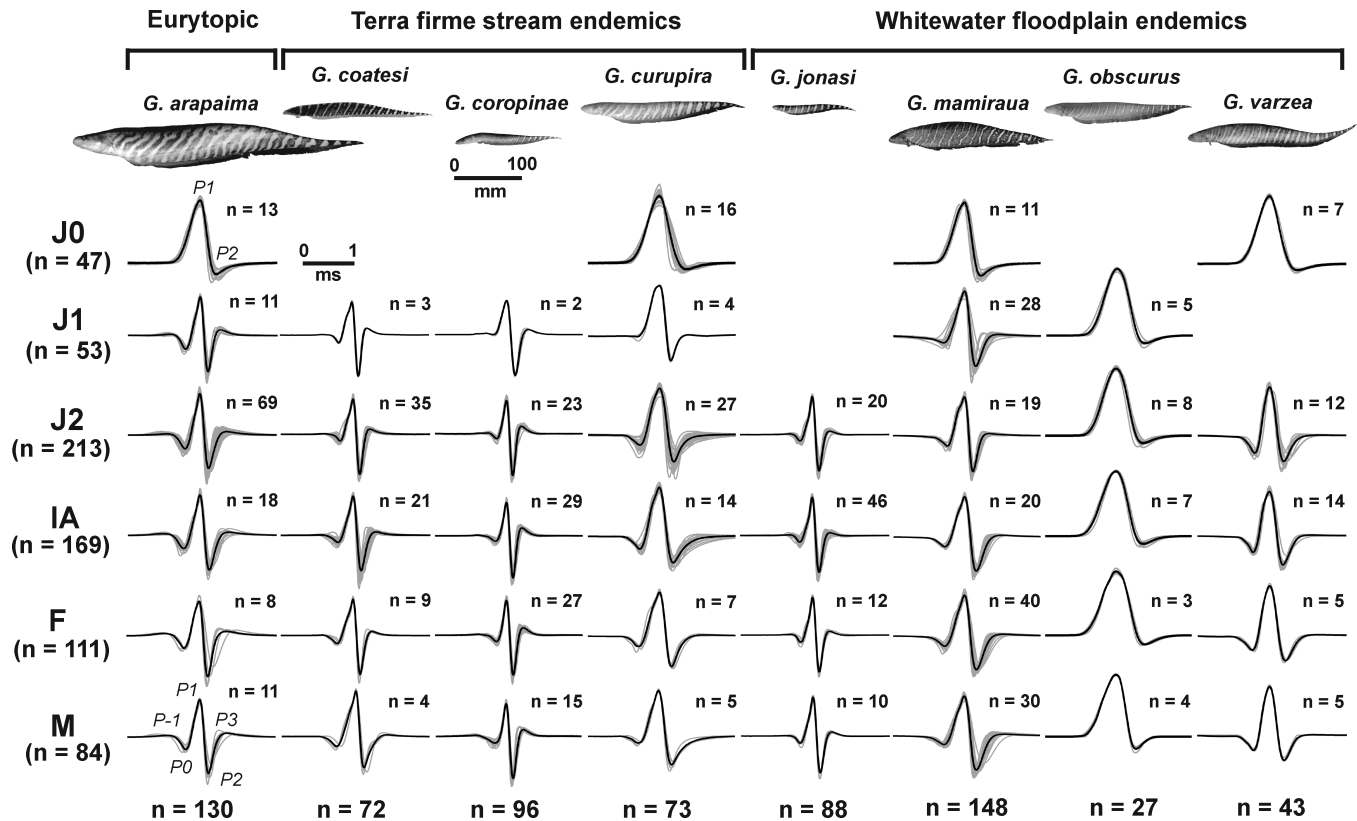
Figure 4. Signal ontogeny of electric organ discharges (EODs) in eight sympatric species of *Gymnotus*. Gray waveforms represent 677 individual recorded fish. Black waveforms are average of all waveforms for a given species-stage. Developmental/maturational stages: J0 = postlarval, J1 = small juvenile, J2 = large juvenile, IA = immature adult, F = mature female, M = mature male. Gaps indicate unavailable recordings. EOD phases are labeled *P*-1 through P3 (see *G. arapaima* J0 and male). For graphical purposes, waveforms are aligned to the P1 peak and normalized to peak-to-peak amplitude. Photographs of live specimens are scaled to the maximum known total length for each species.

measurement for all six heterospecifics (here we excluded *G. obscurus*), and took the mean of these six values. The seven species were then ranked by these means. Note that the use of Mode A measurements would be ineffective for this exercise because, unlike in Mode B, the ontogenetic signal displacement, *j/i*, between a pair of species during an ontogenetic transition, is uninformative of which of a pair of species is moving in signal space.

ASSESSING CONSPICUOUSNESS OF EODs TO ELECTRORECEPTIVE PREDATORS

Some Amazonian piscivores are capable of passive electroreception, including pimelodid catfish, potamotrygonid stingrays, electric eels (*Electrophorus electricus*), and large *Gymnotus* (Stoddard 1999; Crampton 2006). The ampullary electroreceptors of these predators are maximally sensitive around 8 Hz (catfish) to 30 Hz (gymnotiforms) (Stoddard 1999). An assessment of the energy content of a signal at 30 Hz (here termed low-frequency energy, LFE) provides an approximate measure of the conspicuousness of the signal to electroreceptive predators. We used a custom MATLAB program to quantify LFE as signal power (in decibels) in the EOD power density spectrum at 30 Hz.

Results

EOD WAVEFORM DIVERSITY AND ONTOGENY

EOD waveforms from 677 individuals representing eight *Gymnotus* species, and divided into six sex/ontogenetic groups, are presented in Figure 4. In the four species where we were able to record EODs during the J0 postlarval phase, individuals exhibit biphasic EODs comprising a dominant positive phase (P1) followed by a low-amplitude negative phase (P2) (i.e., quasi-monophasic EODs). All species (except *G. obscurus*) exhibit multiphasic (3–5 phase) EODs by the small juvenile (J1) and subsequent stages. *G. obscurus* is exceptional in possessing a biphasic EOD throughout ontogeny. All species represented in Figure 4 exhibit relatively subtle changes during growth and maturation (J1 to adult phases), and male and female EODs are generally similar or indistinguishable. However, *G. coatesi* and *G. curupira* exhibit clear sexual dimorphism in their signals (see Table 2 for distances in signal space between mature males and females of each species). EODs from males of these two species are distinct from those of females and immature adults (the P2 phase is elongated, and in *G. coatesi* the P3 phase is also reduced in amplitude and delayed in onset).
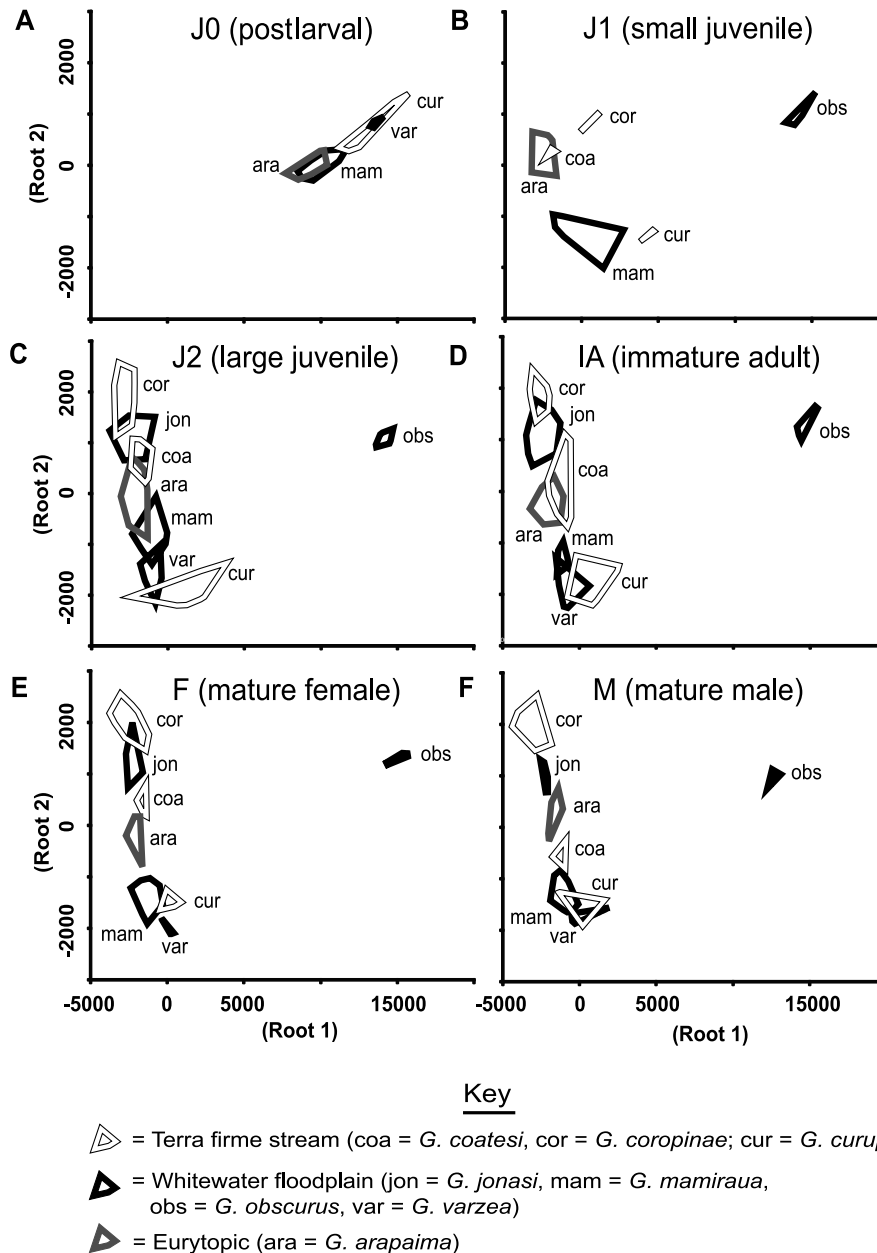
Figure 5. Ordination of the electric organ discharges of eight sympatric species of *Gymnotus* in multivariate signal space by a linear discriminant analysis. Polygons represent the boundaries in signal space for each species, at six ontogenetic stages (A–F).

Sexual dimorphism of EODs has not previously been documented in *Gymnotus*.

ORDINATION OF EODs IN SIGNAL SPACE

In Figure 5, we present two-dimensional representations of signal space, derived from LDA, for each of the six ontogenetic stages. Most of the variability among the 677 EODs is captured by the first two canonical roots, which represent 91.3% and 98.2% of cumulative variance in the dataset, respectively. Each species is represented as a polygon delineating the furthest outlying individuals. During growth, we noted shifts in signal space for many species. At the postlarval stage (J0) there is substantial interspecific overlap of EODs in the area of signal space corresponding to biphasic EODs (Fig. 5A). At the small juvenile (J1) stage, there is dispersion in signal space and a marked shift of all species, except *G. obscurus*, away from the area in signal space corresponding to biphasic EODs (Fig. 5B). During the large juvenile (J2) and immature adult (IA) stages, all species except *G. obscurus* converge into a more restricted area of signal space and exhibit many cases of interspecific overlap (Fig. 5C, D). *Gymnotus obscurus* is a distant outlier in signal space during later ontogeny.
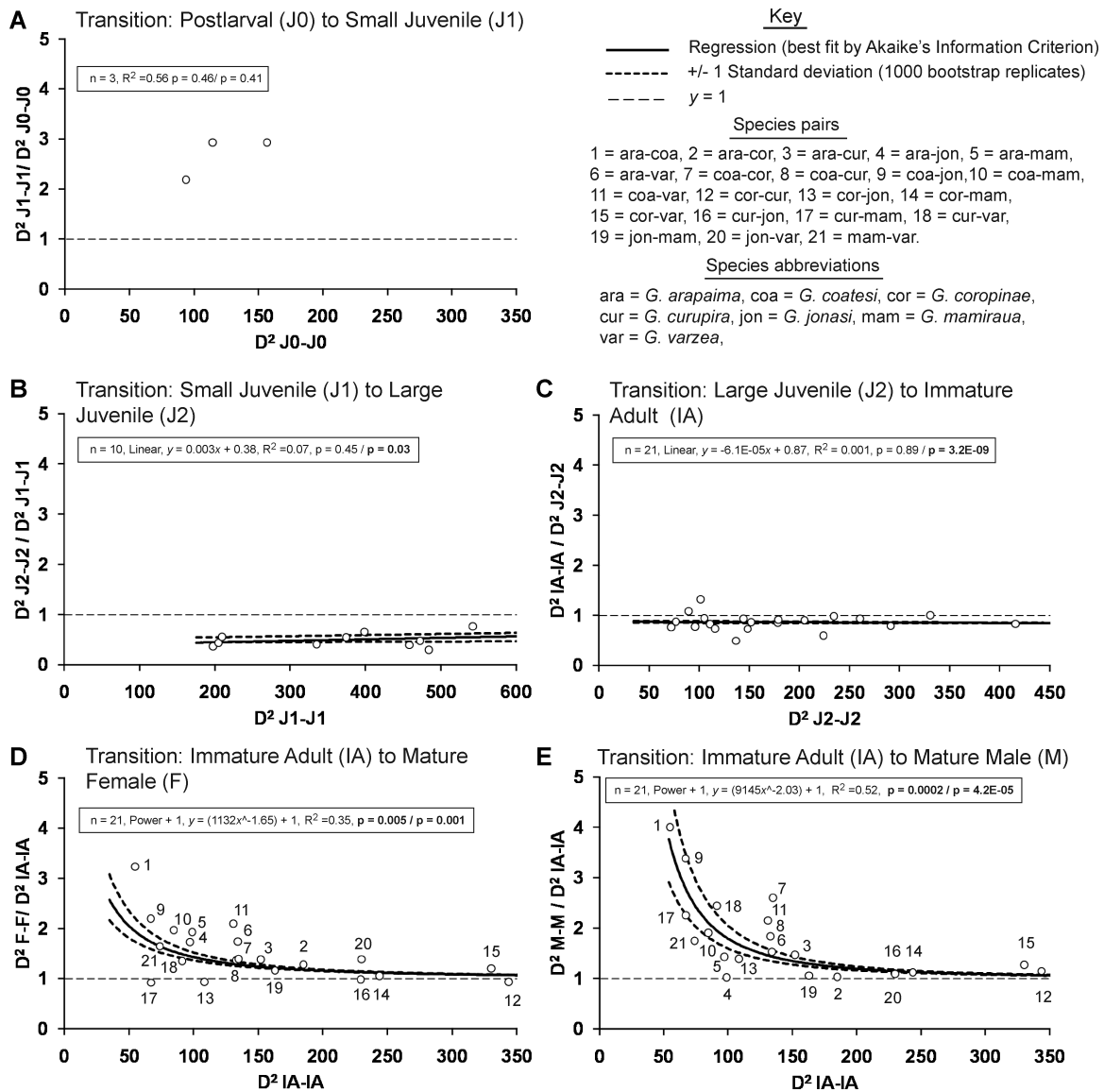
Figure 6. Ontogenetic signal displacement among seven species of *Gymnotus*, during five ontogenetic transitions (A–E) (*G. obscurus* excluded). In each plot the *x*-axis reports *i* (D^2 between a species pair before the ontogenetic transition) and the *y*-axis reports *j/i* (where *j* is D^2 after the transition) for all paired combinations of species (see Fig. 2). Measurements of *i* and *j* follow the Mode A procedure (Fig. 3A). The black solid line illustrates the best-fitted regression to the data, and black dashed lines represent bootstrap confidence intervals at ±one standard deviation from the mean. Boxed text reports: number (*n*) of species pairs; best-fitting function (e.g., Power + 1); R^2 of the regression; *P* values of the regression slope/intercept (significant values reported in bold). Note: a regression line is not fitted to plot A, because both the slope and intercept are nonsignificant.

Finally, in mature specimens, we observed fewer cases of interspecific overlap among males (Fig. 5F), and also females (Fig. 5E), than among immature specimens (Fig. 5A–D). In addition, all cases of overlap among mature specimens involve pairs of species from different habitats (Fig. 5E, F)—a pattern consistent with theoretical expectations from RCD.

THE ONTOGENETIC TEST FOR RCD

Figure 6 reports ontogenetic changes in interspecific signal distances during growth and maturation, based on Mode A measure-

ments in signal space. For each transition, Figure 6 reports the best-fitting function describing the regression between values of *i* (distance in signal space between a species pair prior to an onto-genetic transition) and *j/i* (where *j* = distance in signal space following the transition) (see AIC values in Table S1). The results are remarkably consistent with our theoretical predictions for RCD. During maturation (Fig. 6D, E), but not growth (Fig. 6A–C), values of *i* and *j/i* are negatively correlated and also fit a negative asymptotic power function of the form $j/i = i^{-k} + 1$. This pattern matches our predictions that the more similar two signals are at

Table 1. Analyses of covariance (ANCOVA) for detecting disparities in *j/i* versus the covariate *i* associated with growth and maturation in sympatric *Gymnotus*. For each factor, the corresponding figure is reported.

Model	Factor 1		Factor 2		Intercept			Slope			df
	Transition	Fig.	Transition	Fig.	*P*	Disparity	Bonf.	*P*	Disparity	Bonf.	
1	IA to M	6E	J2 to IA	6C	**<0.0005**	Factor 1>2	**<0.001**	**<0.005**	Factor 1>2	**<0.01**	5,57
1	IA to F	6D	J2 to IA	6C	**<0.01**	Factor 1>2	**<0.01**	**<0.05**	Factor 1>2	**<0.1**	5,57
1	IA to M	6E	IA to F	6D	NS		NS	NS		NS	5,57
2	IA^{Syntopic} to M^{Syntopic}	-	IA^{Allotopic} to M^{Allotopic}	-	NS		NS	NS		NS	2,18*
3	IA^{Syntopic} to F^{Syntopic}	-	IA^{Allotopic} to F^{Allotopic}	-	NS		NS	NS		NS	2,18*

Ontogenetic categories are: J0 = postlarval, J1 = small juvenile, J2 = large juvenile, IA = immature adult, F = mature female, M = mature male. Bold *P* values are significant after sequential Bonferroni (Bonf.) correction (four comparisons—two for model 1, and one each for models 2 and 3). NS = not significant. df = degrees of freedom (∗ = intercept assumes homogeneity of slope).

the immature stage, the further they should be pushed apart by RCD, and also that beyond a safe distance in signal space, selection for additional character displacement should be relaxed (see Fig. 2Dii). The ±1 SD bootstrap confidence intervals also exhibit significant negative asymptotic power functions in Figure 6D,E (see AIC outputs in Table S2), demonstrating the robustness of this function to resampling of the original matrix of DWT coefficients from which the D^2 values were calculated. Using ANCOVA (Table 1), we documented significant disparity of slope and intercept between: (1) the transition from large juveniles to immature adults (late growth), and (2) both the transition from immature adults to mature females, and the transition from immature adults to mature males (maturation). However, we found no significant disparity of slope or intercept between the transition from immature adults to males and the transition from immature adults to females. Thus, although ontogenetic signal displacement attending the maturation of males (Fig. 6E) appears to be greater than in females (Fig. 6D), this difference is not statistically significant.

Before maturation (Fig. 6A–C), we documented an initial period of divergence in signal space during the transition from postlarval specimens to small juveniles (note *j/i* > 1 in Fig. 6A, and see ordinations in Fig. 5A, B). Later, during growth from small to large juveniles (Figs. 6B, 5B, C), we documented a generalized convergence of signals into a more restricted area of signal space, where the amount of displacement (*j/i*) is independent of *i* (yielding a nonsloped linear function, *j/i* < 1). Finally, during growth from large juveniles to immature adults (Figs. 6C, 5C, D), we documented a pattern of stasis in signal space (or slight convergence), consistent with the model in Figure 2C.

CONSPICUOUSNESS OF SIGNAL TRAITS TO ELECTRORECEPTIVE PREDATORS

For all species except *G. obscurus*, which retains high levels of LFE throughout ontogeny, LFE is suppressed by some three orders of magnitude following the transition from biphasic postlarval signals to multiphasic signals, and remains suppressed in later ontogeny (Fig. 7). However, in male *G. coatesi*, *G. curupira*, and *G. varzea*, there is a significant return of LFE relative to immature adults. In these three species, and also in *G. arapaima*, males also exhibit significantly more LFE than females (summary in Table 2C).

Discussion
RCD AMONG MULTIPLE SYMPATRIC SPECIES OF *GYMNOTUS*

Our analyses provide strong support for RCD in the electric signals of *Gymnotus*. During the transition from immature adult individuals to both mature females (Fig. 6D) and males (Fig. 6E), there is a strong negative correlation between the distance separating signals of species at the immature stage (*i*), and the proportional displacement in signal space (*j/i*). This is consistent with theoretical expectations for selection driving signal displacement between pairs of species whose signals are close-by in signal space prior to maturation. Furthermore, the negative correlation between *i* and *j/i* fits the theoretical expectation of a negative asymptotic power function, in which species that are already separated by more than a safe distance in signal space experience negligible selective pressure for additional divergence (see Fig. 6D, E). Importantly, we found that during nonmaturational growth, signal ontogeny did not exhibit patterns consistent with the effects of RCD. We also demonstrated that RCD attends maturation, rather than an increase in body size alone, based on the complete overlap of body size ranges between immature adults and sexually mature adults (Fig. S2). Finally, we also noted that mature specimens exhibit more partitioning in signal space than immature specimens (Fig. 5), an additional expected consequence of RCD.

Based on the evidence summarized above, we have documented a convincing case of RCD among multiple members of a
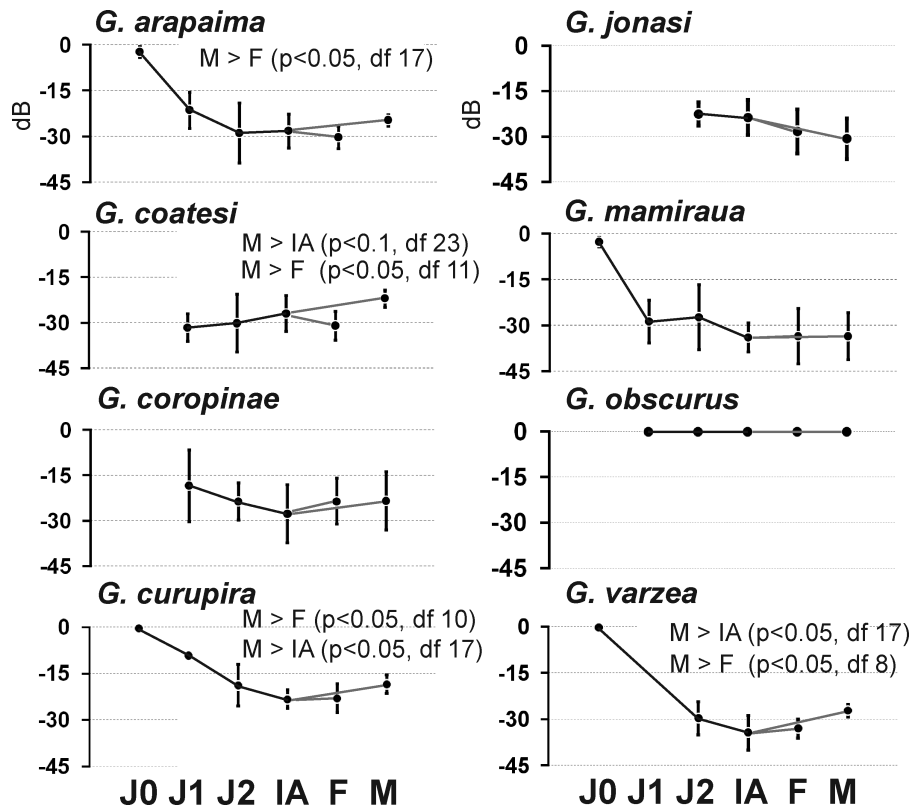
Figure 7. Ontogenetic changes in low-frequency energy, measured as signal power in dB at 30 Hz, for eight sympatric species of *Gymnotus*. Error bars = 1 standard deviation. J0 = postlarval, J1 = small juvenile, J2 = large juvenile, IA = immature adult, F = mature female, M = mature male. Significant disparities between IA, M, and F individuals are reported from two-sample *t*-tests. *P* values follow sequential Bonferroni correction (three comparisons per species).

species-rich assemblage of closely related animals. Unlike in simple two-taxon cases, character displacement between each pair of species in this multispecies community is influenced not just by direct interactions between the pair itself, but also by the positions in signal space of other species in the assemblage. If this were not the case, we would expect some convergences in a cluttered signal space during maturation—that is, the displacement of one pair of species would at least in some cases bring one or both members of this pair closer to the areas of signal space occupied by other sympatric congeners. However, remarkably, not one pair of heterospecific *Gymnotus* that are close-by in signal space as immature adults undergo appreciable convergence during the transition to mature adults (Fig. 6D, E, note no species pairs lie below $j/i = 1$). In sum, the trajectories and magnitudes of character displacement within signal space appear to exhibit a complex interdependence, where each species is simultaneously affected by RCD in relation to several other species.

RCD AMONG ALLOTOPIC VERSUS SYNTOPIC COMBINATIONS OF SPECIES
The costs of mismating should be elevated where opportunities for reproductive interactions are more frequent. Consequently, we

expected that syntopic pairs of species (where both co-occur in the same habitat—either terra firme streams or whitewater floodplains) would exhibit greater signal displacement during maturation than allotopic pairs (where each occurs in a different habitat). However, although mature males and females from syntopic species combinations exhibit fewer instances of overlap in signal space than from allotopic combinations (Fig. 5E, F), ANCOVA recovered no disparity in the magnitude of ontogenetic signal displacement between syntopic and allotopic species pairs (both for males and females) (Table 1, models 2–3). We speculate that the lack of this disparity may be because heterospecific reproductive encounters at the ecotone between terra firme and whitewater floodplain habitats occur frequently enough to drive RCD between allotopic combinations of species.

SIGNAL CHANGES DURING GROWTH, AND THE SUPPRESSION OF LOW-FREQUENCY ENERGY
Our results (summarized in Figs. 5A–D and 6A–C) indicate complex movements of signals through signal space during growth, involving an early stage of divergence (postlarval to small juvenile stages), followed by convergence (small to large juveniles), and then stasis, or slight convergence, in signal space (large juveniles

Table 2. Seven species of *Gymnotus* ranked by: (A) mean strength of ontogenetic signal displacement from sympatric heterospecifics (during maturation) based on Mode B measurements in signal space (see Fig. 3B), and; (B) the magnitude of sexual dimorphism of the EOD, calculated as D^2 from the centroid for EODs of mature males to the centroid for EODs of mature females. We also report (C) significant disparities in low-frequency energy (measured at 30 Hz), which is conspicuous to electroreceptive predators. M/F versus IA compares mature males/females to immature adults. M versus F compares mature males to mature females.

Species	A. Signal displacement from heterospecifics			B. Sexual dimorphism		C. Low-frequency energy	
	Rank	Mean	SD	Rank	D^2 M-F	M/F versus IA	M versus F
Males						M versus IA	
G. coatesi	1	2.335	0.84	1	202.4	**M>IA**	**M>F**
G. curupira	2	1.438	0.45	2	123.0	**M>IA**	**M>F**
G. varzea	3	1.346	0.21	3	49.3	**M>IA**	**M>F**
G. coropinae	4	1.113	0.07	5	46.6	NS	NS
G. arapaima	5	1.112	0.16	6	45.4	NS	**M>F**
G. mamiraua	6	1.052	0.04	7	7.8	NS	NS
G. jonasi	7	1.041	0.05	4	47.3	NS	NS
Females						F versus IA	
G. coatesi	1	1.81	0.35	1	202.4	NS	
G. arapaima	2	1.527	0.24	6	45.4	NS	
G. varzea	3	1.326	0.2	3	49.3	NS	
G. jonasi	4	1.163	0.13	4	47.3	NS	
G. coropinae	5	1.043	0.03	5	46.6	NS	
G. mamiraua	6	0.997	0.04	7	7.8	NS	
G. curupira	7	0.928	0.1	2	123.0	NS	

">" = significantly greater than (reported in bold). NS = no significant disparity (for *P* values see Fig. 7). *Gymnotus obscurus* is excluded here (see justification in Introduction).

to immature adults). A fuller understanding of these movements is beyond the scope of this study and may only be tractable through comparative ontogenetic studies of the physiology of the electric organ and electroreceptors. Here we comment on an interesting feature of signal ontogeny—the suppression of low-frequency signal energy (LFE), which is thought to be conspicuous to electroreceptive predators. Larval and postlarval *Gymnotus* generate monophasic EODs (P1 only), or biphasic EODs with a dominant positive phase (P1) that contain a large component of LFE. These EODs then rapidly shift into multiphasic EODs with a large negative phase and correspondingly low LFE. We argue that the suppression of LFE in immature *Gymnotus* represents a convergent pattern of crypsis, driven by predation on larger specimens by electroreceptive piscivores. In support of this view, Stoddard (1999) and Stoddard and Markham (2008) demonstrated that the appearance of a large negative phase following the P1 phase results in a "cloaking" of LFE, and hypothesized that selection from electroreceptive predators accounts for both the ontogenetic transition from monophasic (or quasi-monophasic) to multiphasic signals, and the evolutionary origin of a multiphasic adult signals from a plesiomorphic monophasic adult condition (but see Lovejoy et al. 2010, and Arnegard et al. 2010b for alternative views of the ancestral condition).

EXCLUDING SENSORY DRIVE AS A MECHANISM FOR SIGNAL DIVERGENCE

The term sensory drive usually describes cases in which the transmission performance of a communication signal is constrained or influenced by the structure of the habitat between sender and receiver (Boughman 2002). Where sympatric species exhibit divergent (or convergent) microhabitat distributions or lifestyles, consequent divergence (or convergence) in signal space can be driven by such physical constraints (e.g., Tobias et al. 2010). Could sensory drive explain the divergence of signals among sympatric *Gymnotus*? The electrosensory system appears to be a prime candidate for sensory drive because electrolocation is the dominant sensory modality involved in prey detection (Albert and Crampton 2005), and because correlations between the dominant frequency of a species' EOD and diet or microhabitat have been predicted (von der Emde and Ringer 1992). However, because selection from the physical environment is not influenced by the distances separating species in signal space, a positive result in our ontogenetic test (i.e., a negative correlation between i and j/i during maturation) cannot be accounted for by sensory drive.

Also, there are reasons to suggest that the head-to-tail EODs of *Gymnotus*, recorded in the far field, may in fact be relatively

unaffected by extrinsic selective pressures from the physical environment. Aguilera et al. (2001) and Rodríguez-Cattaneo et al. (2008) described a hypothesis of caudal/rostral functional specialization in the electric organ (EO) of *Gymnotus*. Caudal portions of the organ generate a strong, "species-specific" far-field EOD component for communication. In contrast, rostral portions of the EO generate a weaker short-range electrolocation carrier signal, which serves mainly to illuminate a cutaneous perioral "electrosensory fovea" of high electroreceptor density. Because of this caudal/rostral specialization, we expect the caudally generated far-field EOD to be relatively unaffected by selective pressures from electrolocation constraints, and thus relatively immune to sensory drive. Moreover, the communication component of EODs may also be relatively immune to sensory drive. Unlike acoustic and visual signals, electrostatic fields are not distorted between sender and receiver by refraction or reflection (Hopkins 1999). Also, unlike acoustic signals, EODs show no frequency-dependent attenuation with distance (Brenowitz 1986).

Finally, long-term field sampling has revealed no obvious correlations between head-to-tail EOD waveform and aspects of the physical environment in *Gymnotus*. For example, the five whitewater floodplain species occur in a remarkably homogenous habitat (floating meadows of macrophytes) with no obvious partitioning of microhabitat or diet, yet exhibit a range of waveforms (biphasic, triphasic, tetraphasic). Likewise, we observed no changes in microhabitat or diet with maturation. Similar observations were reported for a community of mormyrids by Arnegard et al. (2010a).

EXCLUDING MASKING INTERFERENCE AS A MECHANISM FOR SIGNAL DIVERGENCE

Many cases of RCD involving masking interference have been documented from anurans and insects (e.g., Gerhardt and Huber 2002; Amezquita et al. 2006). Could masking interference produce the signal patterns we observed in *Gymnotus*? Coincident pulses of nearby *Gymnotus* can in principle cause masking interference (jamming), because of the close tuning of tuberous electroreceptors to the dominant frequency of the self-generated EOD (Hopkins 1999). However, this is mitigated by a simple behavioral jamming avoidance response (JAR) in which the pulse-repetition rate is altered so as to avoid coincident pulses with neighboring fish (Westby 1979). Because the short EODs of *Gymnotus* represent only a fraction of the duration of the interpulse interval, the JAR is very effective (Westby 1979). Moreover, because the effective range of the EOD for communication is no more than a few body lengths (Hopkins 1988), only nearby fish are likely to promote masking interference in the first place. These circumstances are very different from acoustic signals, which have much greater ranges, and are usually longer in duration (Gerhardt and Huber 2002).

Our results provide additional evidence for the unlikelihood of masking interference in the *Gymnotus* system. If ontogenetic patterns of signal divergence were solely the evolutionary consequence of masking interference, we would expect the dominant frequency of the EOD (Peak Power Frequency, PPF) to exhibit a pattern consistent with RCD—that is, exhibit a significant negative relationship between the predictor i (in this case disparity in PPF between two species at the immature stage) and response j/i (where j = the disparity in PPF between two species following maturation). However, we found no significant correlation between these variables (Pearson's Correlation, $n = 21$, $R^2 = 0.21$, $P = 0.23$). Also, we noted considerable interspecific overlap of PPF ranges among both the mature males and females of *Gymnotus* species from the Tefé region (Fig. S3). These findings appear to rule out masking interference as a significant impetus for RCD.

IS RCD DRIVEN BY REINFORCEMENT OR BY FACILITATED RCD?

Is RCD in *Gymnotus* driven by the costs of hybridization between partially reproductively isolated populations or species, that is, reinforcement, or by the costs of mismating among fully diverged species, that is, facilitated RCD? We found no evidence for ongoing hybridization among *Gymnotus* from the Tefé area, in the form of intermediate EODs or morphology. Also, phylogenetic and biogeographic studies (Albert et al. 2004; Lovejoy et al. 2010) indicate that *Gymnotus* did not diversify rapidly, in geographically localized species flocks. On the contrary, local assemblages of *Gymnotus*, including that of the Tefé area, comprise nonmonophyletic collections of genetically distinct species (Albert et al. 2004; Lovejoy et al. 2010), many of which exhibit very broad distributions (Crampton 2011). This implies that the *Gymnotus* fauna of the Tefé region was assembled incrementally, and slowly, from a continental-scale species pool, rather than via rapid in-situ diversification (Crampton 2011). Under these circumstances, RCD is best interpreted as a predominantly postspeciation phenomenon driven by the costs of mismating among fully divergent species (facilitated RCD), and not by selection against hybridization in incipient species (reinforcement).

CORRELATIONS OF ONTOGENETIC SIGNAL DISPLACEMENT BETWEEN SEXES

We noted a pattern consistent with RCD during the maturation of both females and males (Fig. 6D, E, Table 1). Moreover, based on Mode B measurements, we documented a weak but strongly significant positive correlation between the magnitude of ontogenetic signal displacement from heterospecifics in females (j/i in transition from immature adults to females), and the magnitude of ontogenetic signal displacement from heterospecifics in males (j/i in transition from immature adults to males) (Pearson's correlation, $n = 42$. $R^2 = 0.38$, $P < 0.0001$; Fig. S4). This correlation

has two plausible explanations. First, it may indicate two-way mate choice, where males choose females on the basis of their EODs and vice versa. Many animal mate attraction signals are generated only by males (e.g., anurans, birds), but electric fish EODs are generated by both sexes—allowing the possibility for two-way mate choice. Indeed, playback experiments have demonstrated that mormyrid electric fish exhibit both male and female mate choice (Arnegard et al. 2006; Feulner et al. 2009). Further, *Gymnotus* undertakes extended paternal care of eggs and young (Crampton and Hopkins 2005), and paternal care usually predicts an increased role for male selection of females (Clutton-Brock 1991). Alternatively (or additionally), the positive correlation between the strength of RCD in males and females could stem from a (largely) autosomally driven genetic correlation in signal traits between the sexes (Fisher 1958).

SEXUAL DIMORPHISM AND SEXUAL SELECTION OF EODs

We observed sexual dimorphism of EODs in some *Gymnotus* species, accompanied by a male exaggeration of LFE—a signal trait that is likely costly because it increases conspicuousness to electroreceptive predators. This exaggeration of LFE contrasts with its suppression from early ontogenetic stages during growth (Fig. 7). Sexual dimorphism of signals is known from other gymnotiform genera where it usually also involves the exaggeration of signal components that are conspicuous to predators or energetically demanding, and that are suppressed in immature specimens (notably in *Brachyhypopomus* and *Sternopygus*, see Crampton and Albert 2006; Salazar and Stoddard 2008; Stoddard and Markham 2008). Costly, ornamental, signal traits in male animals are commonly favored by sexual selection (i.e., attractive to females) in spite of, or even because of these costs, because they represent honest indices of male quality (i.e., "handicaps" sensu Zahavi 1977).

Here we propose that sexual selection and RCD may interact to promote the divergence of signal traits (and associated female preferences) among sympatric taxa (see Endler 1989; Ryan and Rand 1993; Higgie and Blows 2007). Males of the three species exhibiting the greatest magnitude of sexual dimorphism in EODs (i.e., *G. coatesi, G. curupira, G. varzea*, Table 2B), and also the most prominent expression of costly signal traits, that is, LFE (Table 2C), exhibit the highest average magnitude of ontogenetic signal displacement from heterospecifics (Table 2A). Likewise, summed over seven species, the magnitude of ontogenetic signal displacement from heterospecifics (in males) is positively correlated to the magnitude of sexual dimorphism (Pearson's Correlation, $R^2 = 0.89$, $P < 0.001$). This correlation supports the notion that the design of signals is under simultaneous selective pressure from the costs of mismating (which drives RCD) and from sexual selection (which leads to sexual dimorphism of signals).

What explains the correlation between ontogenetic signal displacement and sexual dimorphism? We believe that sexual selection alone cannot explain the patterns of signal divergence during maturation that we have observed in the Tefé *Gymnotus* assemblage. First, if sexual selection were the sole impetus for signal divergence, there would be no expectation that the distance between two species in signal space at the immature stage (i) should be negatively correlated to the displacement of signals during maturation (j/i). In other words, sexual selection can drive the evolution of conspicuous, dimorphic signals, but it cannot alone explain why these should also be divergent among species in a manner that would reduce errors in recognition and mating. Second, consider the case of two fully divergent species coming into reproductive contact following a history of allopatric speciation and geographical dispersal. When this occurs, there is no reason that sexual selection of costly signal traits should be heightened in one or both of these species. In contrast, there are ample grounds to predict heightened selection for signal displacement if the two species possess similar signals. We therefore hypothesize that the correlation we have documented between the magnitude of ontogenetic character displacement and the magnitude of sexual dimorphism arose because RCD catalyzes heightened sexual selection following reproductive contact. In turn, this opens a pathway for rapid divergence of signals among males, hence minimizing the risk of interspecific mismating while simultaneously promoting sexually dimorphic signals. In other words, heightened sexual selection of costly signal traits may be initiated as a consequence of RCD, but thereafter the two processes act in concert.

Studies from species flocks have suggested that sexual selection may play a leading role in driving signal divergence among incipient species, leading to consequent reproductive isolation and speciation (e.g., Boughman 2001; Allender et al. 2003; Mendelson and Shaw 2005; Boul et al. 2007; Arnegard et al. 2010a). In species flocks, signal divergence may occur concomitantly with speciation, and so sexual selection, in theory, can lead to interspecific signal divergence in sympatry, without the need to invoke reinforcement on secondary contact (Pomiankowski and Iwasa 1998). However, local assemblages of *Gymnotus* do not exhibit evidence of recent in situ speciation. On the contrary, as outlined above, signal divergence in *Gymnotus* is likely a strictly postspeciation phenomenon, driven predominantly by facilitated RCD following reproductive contact between fully divergent species (with sexual selection playing an additional role as discussed above).

COMMUNITY-WIDE SIGNAL PARTITIONING AND THE INTERACTION OF RCD AND SEXUAL SELECTION

We suggest that cases of community-wide RCD resembling that of *Gymnotus*, and driven specifically by the costs of mismating (rather than masking interference), may be common. For

example, several other electric fish groups, including mormyrids, exhibit community-wide signal partitioning, and a signal ontogeny in which mature males of some (but not all) species exhibit conspicuous or energetically costly signals relative to females and immature specimens (e.g., Bass 1986; Arnegard and Hopkins 2003; Arnegard et al. 2005; Crampton and Albert 2006). Some visual communication systems exhibit similar patterns and may also submit to mapping into multivariate signal space (see Endler et al. 2005). For instance, Lake Malawi cichlids (Konings 2001), and several groups of birds, for example, *Anas, Dendroica,* and Emberizidae (Sibley 2003), exhibit a signal ontogeny in which juveniles and mature females have cryptic coloration (presumably in response to predation) and are notoriously hard to distinguish among species. In contrast, mature males exhibit conspicuous nuptial color patterns (from homologous precursor patterns in immature stages) that are highly distinct across sympatric species. As in the *Gymnotus* system, selection for cryptic signal design may be disrupted during maturation by RCD among heterospecifics, and also by sexual selection for conspicuous male secondary sexual ornaments.

The mechanisms by which RCD and sexual selection interact to generate signals that are simultaneously attractive to the opposite sex, and species-specific, are poorly understood (Endler 1989; Ryan and Rand 1993; Higgie and Blows 2007)—in part because evolutionary studies of mate attraction signals have placed more emphasis on sexual selection, but also because of the difficulty of testing for and recognizing RCD outside two-taxon cases. In this study, we have provided evidence to suggest that on reproductive contact in sympatry, RCD may act as a catalyst for heightened sexual selection. This subject deserves future attention, especially because of its relevance to studies of reproductive isolation and speciation, where the roles of sexual selection and RCD are hard to disentangle (e.g., Mendelson and Shaw 2005; Leal and Losos 2010). Further studies of the dynamics of RCD in multispecies communities, including those which explore signal ontogeny, will likely yield important insights into animal diversification.

LITERATURE CITED
Aguilera, P. A., M. E. Castello, and A. A. Caputi. 2001. Electroreception in *Gymnotus carapo*: differences between self-generated and conspecific-generated signal carriers. J. Exp. Biol. 204:185–198.

Albert, J. S, and W. G. R. Crampton. 2005. Electroreception and electrogenesis. Pp. 431–472 *in* D. Evans, ed. The physiology of fishes. 3rd ed. C.R.C. Press, New York.

Albert, J. S., W. G. R. Crampton, D. H. Thorsen, and N. R. Lovejoy. 2004. Phylogenetic systematics and historical biogeography of the Neotropical electric fish *Gymnotus* (Gymnotidae: Teleostei). Syst. Biodivers. 2:375–417.

Allender, C. J., O. Seehausen, M. E. Knight, G. F. Turner, and N. Maclean. 2003. Divergent selection during speciation of Lake Malawi cichlid fishes inferred from parallel radiations in nuptial coloration. Proc. Natl. Acad. Sci. USA 100:14074–14079.

Amezquita, A., W. Hodl, A. P. Lima, L. Castellanos, L. Erdtmann, and M. C. De Araujo. 2006. Masking interference and the evolution of the acoustic communication system in the Amazonian dendrobatid frog *Allobates femoralis*. Evolution 60:1874–1887.

Arnegard, M. E., and C. D. Hopkins. 2003. Electric signal variation among seven blunt-snouted *Brienomyrus* species (Teleostei: Mormyridae) from a riverine species flock in Gabon, Central Africa. Environ. Biol. Fishes 67:321–339.

Arnegard, M. E., S. M. Bogdanowicz, and C. D. Hopkins. 2005. Multiple cases of striking genetic similarity between alternate electric fish signal morphs in sympatry. Evolution 59:324–343.

Arnegard, M. E., B. S. Jackson, and C. D. Hopkins. 2006. Time-domain signal divergence and discrimination without receptor modification in sympatric morphs of electric fishes. J. Exp. Biol. 209:2182–2198.

Arnegard, M. E., P. B. McIntyre, L. J. Harmon, M. L. Zelditch, W. G. R. Crampton, J. K. Davis, J. P. Sullivan, S. Lavoué, and C. D. Hopkins. 2010a. Sexual signal evolution outpaces ecological divergence during electric fish species radiation. Am. Nat. 176:335–356.

Arnegard, M. E., D. J. Zwickl, Y. Lu, and H. H. Zakon. 2010b. Old gene duplication facilitates origin and diversification of an innovative communication system—twice. Proc. Natl. Acad. Sci. USA 107:22172–22177.

Bass, A. H. 1986. A hormone-sensitive communication system in an electric fish. J. Neurobiol. 17:131–156.

Boughman, J. W. 2001. Divergent sexual selection enhances reproductive isolation in sticklebacks. Nature 411:944–948.

———. 2002. How sensory drive can promote speciation. Trends Ecol. Evol. 17:571–577.

Boul, K. E., W. C. Funk, C. R. Darst, D. C. Cannatella, and M. J. Ryan. 2007. Sexual selection drives speciation in an Amazonian frog. Proc. R. Soc. Lond. B. Biol. Sci. 274:399–406.

Brenowitz, E. A. 1986. Environmental influences on acoustic and electric animal communication signals. Brain, Behav. Evol. 28:32–42.

Bullock, T. H., C. D. Hopkins, A. N. Popper, and R. R. Fay. 2005. Electroreception. Springer, New York.

Butlin, R. K. 1995. Reinforcement: an idea evolving. Trends Ecol. Evol. 10:432–434.

Butlin, R. K., and M. G. Ritchie. 1994. Mating behaviour and speciation. Pp. 43–79 *in* P. J. B. Slater and T. R. Halliday, eds. Behaviour and speciation. Cambridge Univ. Press, Cambridge.

Chek, A. A., B. P. Bogart, and S. C. Lougheed. 2003. Mating signal partitioning in multi-species assemblages: a null model test using frogs. Ecol. Lett. 6:235–247.

Cherry, L. M., S. M. Case, J. G. Kunkel, J. S. Wyles, and A. C. Wilson. 1982. Body shape metrics and organismal evolution. Evolution 36:914–933.

Clutton-Brock, T. H. 1991. The evolution of parental care. Princeton Univ. Press, Princeton, NJ.

Cooley, J. R. 2007. Decoding asymmetries in reproductive character displacement. Proc. Acad. Nat. Sci. Philadelphia 156:89–96.

Crampton, W. G. R. 2006. Evolution of electric signal diversity in gymnotiform fishes. II. Signal design. Pp. 697–731 *in* F. Ladich, S. P. Collin, P. Moller, and B. G. Kapoor, eds. Communication in fishes. Science Publishers, Enfield, NH.

———. 2011. An ecological perspective on diversity and distributions. Pp. 165–189 *in* J. S. Albert and R. E. Reis, eds. Historical biogeography of Neotropical freshwater fishes. Univ. California Press, Berkeley, CA:

Crampton, W. G. R., and J. S. Albert. 2006. Evolution of electric signal diversity in gymnotiform fishes. I. Phylogenetic systematics, ecology and biogeography. Pp. 647–696; 718–731 *in* F. Ladich, S. P. Collin, P. Moller, and B. G. Kapoor, eds. Communication in fishes. Science Publishers, Enfield, NH.

Crampton, W. G. R., and C. D. Hopkins. 2005. Nesting and paternal care in the weakly electric fish *Gymnotus* (Gymnotiformes: Gymnotidae) with descriptions of larval and adult electric organ discharges of two species. Copeia 2005:48–60.

Crampton, W. G. R., J. K. Davis, N. R. Lovejoy, and M. Pensky. 2008. Multivariate classification of animal communication signals: a simulation-based comparison of alternative signal processing procedures using electric fishes. J. Physiol. Paris 102:304–321.

Endler, J. A. 1989. Conceptual and other problems in speciation. Pp. 625–648 *in* D. Otte and J. A. Endler, eds. Speciation and its consequences. Sinauer, Sunderland, MA.

Endler, J. A., D. A. Westcott, J. R. Madden, and T. Robson. 2005. Animal visual systems and the evolution of color patterns: sensory processing illuminates signal evolution. Evolution 59:1795–1818.

Feulner, P. G. D., F. Kirschbaum, C. Schugardt, V. Ketmaier, and R. Tiedemann. 2006. Electrophysiological and molecular genetic evidence for sympatrically occurring cryptic species in African weakly electric fishes (Teleostei: Mormyridae: *Campylomormyrus*). Mol. Phylogenet. Evol. 39:198–208.

Feulner, P. G. D., M. Plath, J. Engelmann, F. Kirschbaum, and R. Tiedemann. 2009. Electrifying love: electric fish use species-specific discharge for mate recognition. Biol. Lett. 5:225–228.

Fisher, R. 1958. The genetical theory of natural selection. 2nd edition. Clarendon Press, Oxford, UK.

Gerhardt, H. C. 1999. Reproductive character displacement and other sources of selection on acoustic communication systems. Pp. 515–534 *in* M. D. Hauser, and M. Konishi, eds. The design of animal communication. MIT Press, Cambridge, MA.

Gerhardt, H. C., and F. Huber. 2002. Acoustic communication in insects and anurans: common problems and diverse solutions. The Univ. of Chicago Press, Chicago.

Gröning, J., and A. Hochkirch. 2008. Reproductive interference between animal species. Q. Rev. Biol. 83:257–282.

Higgie, M., and M. W. Blows. 2007. Are traits that experience reinforcement also under sexual selection? Am. Nat. 170:409–420.

Hopkins, C. D. 1988. Neuroethology of electric communication. Ann. Rev. Neurosci. 11:497–535.

———. 1999. Signal evolution in electric communication. Pp. 461–491 *in* M. D. Hauser, and M. Konishi, eds. The design of animal communication. MIT Press, Cambridge, MA.

Howard, D. J. 1993. Reinforcement: origin, dynamics, and fate of an evolutionary hypothesis. Pp. 46–69 *in* R. Harrison, ed. Hybrid zones and the evolutionary process. Oxford Univ. Press, New York.

Konings, A. 2001. Malawi cichlids in their natural habitat. 3rd edition. Cichlid Press, El Paso.

Leal, M., and Losos, J. B. 2010. Communication and speciation. Nature 467:159–160.

Lemmon, E. M. 2009. Diversification of conspecific signals in sympatry: geographic overlap drives multidimensional reproductive character displacement in frogs. Evolution 63:1155–1170.

Lovejoy, N. R., K. Lester, W. G. R. Crampton, F. P. L. Marques, and J. S. Albert. 2010. Phylogeny, biogeography, and electric signal evolution of Neotropical knifefishes of the genus *Gymnotus* (Pisces: Gymnotidae). Mol. Phylogenet. Evol. 54:278–290.

Luddecke, H., A. Amezquita, X. Bernal, and F. Guzman. 2000. Partitioning of vocal activity in a Neotropical highland-frog community. Stud. Neotrop. Fauna Environ. 35:185–194.

Luther, D. A., and R. H. Wiley. 2009. Production and perception of communicatory signals in a noisy environment. Biol. Lett. 5:183–187.

Mahalanobis, P. C. 1936. On the generalized distance in statistics. Proc. Nat. Inst. Sci. India 2:49–55.

Mayr, E. 1988. The why and how of species. Biol. Phil. 3:431–441.

Mendelson, T. C., and K. L. Shaw. 2005. Rapid speciation in an arthropod. Nature 433:375–376.

Nelson, D. A. 1989. The importance of invariant and distinctive features in species recognition of bird song. Condor 91:120–130.

Nelson, D. A., and P. Marler. 1990. The perception of birdsong and an ecological concept of signal space. Pp. 443–478 *in* W. C. Stebbins, and M. A. Berkley, eds. Comparative perception. Vol. II. Complex Signals. J. Wiley, New York, NY.

Noor, M. A. F. 1999. Reinforcement and other consequences of sympatry. Heredity 83:503–508.

Otte, D. 1994. The crickets of Hawaii: origin, systematics and evolution. The Orthopterist's Society, Philadelphia, PA.

Pereira, A. C., A. Rodríguez-Cattaneo, M. E. Castello, and A. A. Caputi. 2007. Post-natal development of the electromotor system in a pulse gymnotid electric fish. J. Exp. Biol. 210:800–814.

Pfennig, K. S., and D. W. Pfennig. 2009. Character displacement: ecological and reproductive responses to a common evolutionary problem. Q. Rev. Biol. 84:253–276.

Podos, J. 2001. Correlated evolution of morphology and vocal signal structure in Darwin's finches. Nature 409:185–188.

Pomiankowski, A., and Y. Iwasa. 1998. Runaway ornament diversity caused by Fisherian sexual selection. Proc. Natl. Acad. Sci. USA 95:5106–5111.

Rodríguez-Cattaneo, A., A. C. Pereira, P. A. Aguilera, W. G. R. Crampton, and A. A. Caputi. 2008. Species-specificity of a fixed motor pattern: the electric organ discharge of *Gymnotus*. PLOS One 3:1–13.

Ryan, M. J. 1985. The tungara frog: a study in sexual selection and communication. Univ. of Chicago Press, Chicago.

Ryan, M. J., and A. S. Rand. 1993. Species recognition and sexual selection as a unitary problem in animal communication. Evolution 47:647–657.

Salazar, V. L., and P. K. Stoddard. 2008. Sex differences in energetic costs explain sexual dimorphism in the circadian rhythm modulation of the electrocommunication signal of the gymnotiform fish *Brachyhypopomus pinnicaudatus*. J. Exp. Biol. 211:1012–1020.

Seehausen, O., Y. Terai, I. S. Magalhaes, K. L. Carleton, H. D. J. Mrosso, R. Miyagi, I. Van Der Sluijs, M. V. Schneider, M. E. Maan, H. Tachida, et al. 2008. Speciation through sensory drive in cichlid fish. Nature 455:620–623.

Servedio, M. R., and M. A. F. Noor. 2003. The role of reinforcement in speciation: theory and data. Ann. Rev. Ecol. Evol. Syst. 34:339–364.

Sibley, D. 2003. Field guide to the birds of eastern North America. Christopher Helm, London, U.K.

Stoddard, P. K. 1999. Predation enhances complexity in the evolution of electric fish signals. Nature 400:254–256.

Stoddard, P. K., and M. R. Markham. 2008. Signal cloaking by electric fish. Bioscience 58:415–425.

Tobias, J. A., J. Aben, R. T. Brumfield, E. P. Derryberry, W. Halfwerk, H. Slabbekoorn, and N. Seddon. 2010. Song divergence by sensory drive in Amazonian birds. Evolution. 64:2820–2839.

von der Emde, G., and T. Ringer. 1992. Electrolocation of capacitive objects in four species of pulse-type weakly electric fish. I. Discrimination performance. Ethology 91:326–338.

Westby, G. W. M. 1979. Electrical communication and jamming avoidance between resting *Gymnotus carapo*. Anim. Behav. 23:192–213.

Wollerman, L. 1999. Acoustic interference limits call detection in a Neotropical frog *Hyla ebraccata*. Anim. Behav. 57:529–536.

Zahavi, A. 1977. The cost of honesty (further remarks on the handicap principle). J. Theor. Biol. 67:603–605.

Supporting Information

The following supporting information is available for this article:

Table S1. Model fitting with AIC for regression of predictor *i* versus response *j/i* in Figure 6 A–E (all ontogenetic transitions).

Table S2. Model fitting with AIC for regression of predictor *i* versus response *j/i* in Figure 6 D–E (transition from immature adults to: D. mature females; E. mature males).

Figure S1. Map of Tefé area, Brazil, showing sampling areas and major habitat types.

Figure S2. Ranges of total lengths for eight species of *Gymnotus* at six ontogenetic stages.

Figure S3. Peak power frequency ranges for EODs of mature male and females of eight species of *Gymnotus*.

Figure S4. Correlation of the magnitude of ontogenetic signal displacement attending maturation between males and females of seven species of *Gymnotus*.

Appendix S1. Modified Nikolsky-scale of gonadal development for *Gymnotus*.

Appendix S2. Defining length cut-offs in ontogenetic stages of *Gymnotus*.

Appendix S3. Additional methods for signal recording.

Appendix S4. Generating characters from electric fish EODs for measuring mahalanobis distances: the discrete wavelet transform.

Supporting Information may be found in the online version of this article.

Please note: Wiley-Blackwell is not responsible for the content or functionality of any supporting information supplied by the authors. Any queries (other than missing material) should be directed to the corresponding author for the article.